Long-time dynamics of the directional solidification of rodlike eutectics

Mikaël Perrut, Silvère Akamatsu, Sabine Bottin-Rousseau,* and Gabriel Faivre
Institut des Nanosciences de Paris, CNRS UMR 7588, Université Pierre-et-Marie-Curie, Campus Boucicaut, 140 rue de Lourmel, 75015 Paris, France

(Received 10 September 2008; published 17 March 2009)

We report long-duration real-time observations of the dynamics of hexagonal (rodlike) directional-solidification patterns in bulk samples of a transparent eutectic alloy. A slight forward curvature of the isotherms induces a slow dilatation of the growth pattern at constant solidification rate and triggers the rod-splitting instability. At long times, the rod-splitting frequency exactly balances the dilatation driven by the curved isotherms. The growth pattern is then disordered and nonstationary but has a sharply selected mean spacing. Well-ordered growth patterns can be grown using time-dependent solidification rates.

DOI: 10.1103/PhysRevE.79.032602 PACS number(s): 81.10.Aj, 81.30.Fb, 47.54.−r, 61.05.−a

Directional solidification of nonfaceted binary eutectics (i.e., binary alloys, which are two-phased in the solid state, both solid phases displaying nonfaceted melt growth) gives rise to diffusion-controlled out-of-equilibrium patterns consisting of more or less periodic arrangements of the two solid phases over the solid-liquid interface. These patterns can be either lamellar (periodic in one direction) or rodlike (forming hexagonal arrays). They have spacing values, which, in order of magnitude, vary with the solidification rate V as $V^{-0.5}$, are of a few micrometers in the $0.1-10$ μm s^{-1} V range, and thus contain large numbers of repeat units in bulk samples. The stability of these patterns and other aspects of their nonlinear dynamics have been fundamental research subjects for decades. Much progress has been made, but our current knowledge still has important deficiencies [1]. In this communication, we focus on the question of the long-time dynamics of eutectic growth fronts (i.e., their behavior at arbitrary long solidification times) at given V and alloy composition. This question, although central in elaboration of metallic materials, has not yet been solved essentially for lack of well-resolved methods of *in situ* observation of solidification fronts. *Postsolidification* metallographic analyses have set the framework, but could not clarify the dynamical nature nor explain the apparent uniqueness (as opposed to initial condition dependence) of eutectic growth patterns at long solidification times. Briefly stated, the conclusion of the metallurgical studies is that some statistical features of eutectic growth patterns (mostly, their mean spacing $\bar{\lambda}$ and the width of their λ distribution [2]) settle down to constant, reproducible values after long solidification times at fixed V. On the other hand, it is now well established that, in ideal (unbounded, isotropic) systems, periodic eutectic growth patterns have finite-width stability intervals of λ, which implies that any periodic growth pattern belonging to this interval can be created by an appropriate choice of the solidification programs, and then maintained indefinitely at fixed V [3,4]. In this Brief Report, we report on experiments that clarify how the metallurgical results can be reconciled with the predicted "multistability" of eutectic growth.

We have performed real-time optical observations of directional-solidification fronts in bulk samples of a transparent rodlike eutectic alloy, namely, succinonitrile-(d)camphor (SCN-DC) at eutectic concentration (14 mol % of DC). Such observations allow an accurate spatiotemporal study of the entire growth pattern, which is unprecedented in bulk samples. The experimental methods that we used have been explained in detail previously [5]. In brief, flat glass crucibles of internal cross section 0.4×6 mm^2 are filled with eutectic SCN-DC and placed between a cold oven and a hot oven. A thermal gradient G of 8 ± 1 K mm^{-1} is established by diffusion along the sample. The sample is then pulled at a rate V toward the cold oven. During the pulling, the envelope of the growth front remains locked onto the isotherm at the eutectic temperature T_E (38.3 °C) of SCN-DC. On a smaller scale, it exhibits growth patterns consisting of arrays of DC caps embedded in a continuous SCN matrix. Previous studies confirmed that the mean spacing of these patterns obeys the usual scaling law of eutectic growth, i.e., it remains close to the minimum-undercooling spacing for two-dimensional eutectic growth λ_m [6], which, in the case of SCN-DC, is given by $\lambda_m^2 V = 10.2 \pm 1.5$ μm^3 s^{-1} [7]. Our method of observation yields dark-field images of these patterns, in which a bright spot is associated with each DC cap (Fig. 1). These images are digitized and stored in a computer, and then processed to

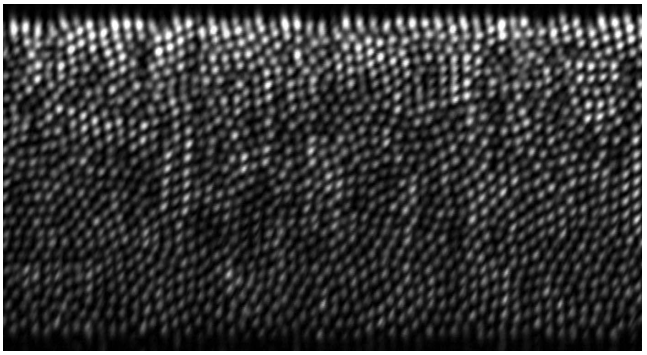

FIG. 1. Growth front of the rodlike eutectic alloy SCN-DC directionally solidified at $V=0.035$ μm s^{-1}. The growth direction **z** is pointing toward the reader. The bright spots are the caustics of the light rays transmitted by the curved DC-liquid interfaces (see Fig. 3). The upper and lower edges of the image are 400 μm apart and correspond to the contact lines of the front and the crucible walls.

*bottin@insp.jussieu.fr

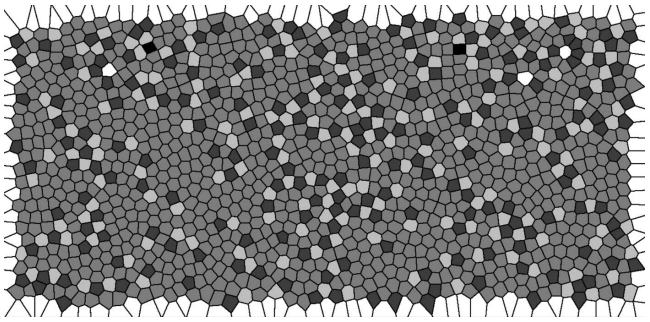

FIG. 2. Voronoi diagram of the growth pattern of Fig. 1. Hexagons: medium gray. Pentagons: light gray. Heptagons: dark gray.

yield Voronoi diagrams (Fig. 2), or binarized diagrams, in which each DC cap is represented by its center of mass (Fig. 3). We used the former to visualize the topological defects of the hexagonal patterns and the latter to study the trajectories of their individual repeat units. The resolution limit (≈ 3 μm) of this method of observation is well below the observed spacing values in the explored V range (0.01 to 0.06 μm s^{-1}). During this study, weakly anisotropic single eutectic grains were grown, as explained in Ref. [8].

Recording the trajectories of the DC caps during long-duration solidification runs, we found that the DC caps were slowly but continually drifting to the sample walls, where they were eventually terminated (Fig. 3). The drift was not uniform, and thus could not be ascribed to a misalignment of the thermal gradient with respect to the growth axis **z**. Reproducibly, the drift velocity V_d varied monotonically with the coordinate y along the normal to the sample walls, and changed sign at a position y_o, which varied from experiment to experiment. Thus the growth patterns were undergoing a permanent stretching in the **y** direction. No drift parallel to the walls was observed. A simple explanation for this observation is that, in our experiments, the T_E isotherm had a forward (bulging into the liquid) curvature in the **yz** plane perpendicular to the walls, but none in the plane parallel to the walls, and that the trajectories of the DC caps remained perpendicular to this isotherm in virtue of the well-known "normal-growth" semiempirical rule, as shown in Fig. 3.

According to this rule, the local drift velocity of a growth pattern due to a unidirectional curvature of the isotherms is

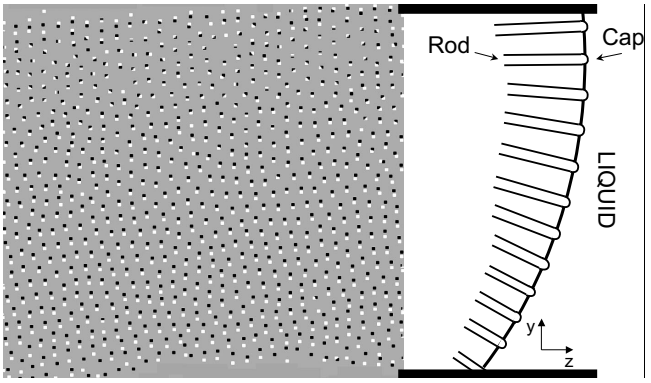

FIG. 3. Left: Superposition of two binarized micrographs of a growth pattern at times t_1 (black dots) and t_1+30 min (white dots). $V=0.035$ μm s^{-1}. Vertical dimension: 400 μm. Right: Sketch of a longitudinal section of the system assuming a (largely exaggerated) forward curvature of the growth front.

given by $V_d(y)=V\partial\zeta/\partial y$, where $z=\zeta(y)$ is the equation of a longitudinal section of the T_E isotherm. The measured values of V_d varied linearly with y within the experimental uncertainty. Taking the **y** axis origin at equal distance from the two glass plates, we may write $\partial\zeta/\partial y=\tan\alpha_o - y/R$ and $y_o = R\tan\alpha_o$, where $1/R$ is the curvature of the isotherm at $y=y_o$, and α_o a (residual) thermal misalignment angle (smaller than 3°) in the **yz** plane [5]. We found that R was always much larger than the sample thickness, remained constant during a given solidification run, but could vary from run to run. Values of R measured in nine samples for different values of V ranged from about 2.2 to 5.4 mm (in Fig. 3, $R\approx 4.4$ mm and $\alpha_o \approx 2.1°$). The differences in R were not correlated with differences in V, and were thus most probably due to (unwanted) changes in the ambient conditions affecting the thermal field inside the sample. We also calculated R from the rate of increase of $\bar{\lambda}$ over time. An elementary geometrical calculation shows that, for a uniform one-directional curvature R^{-1} of the T_E isotherm, $\bar{\lambda}(t)\approx\bar{\lambda}_o e^{t/\tau}$, where $\tau = 2R/V$ and $\bar{\lambda}_o$ is the value of $\bar{\lambda}$ at $t=0$. This equation is valid when the number of repeat units is locally conserved, i.e., when no DC cap is created or terminated during the process. DC-cap terminations were not observed during this study except at the sample walls. DC-cap creation events called rod

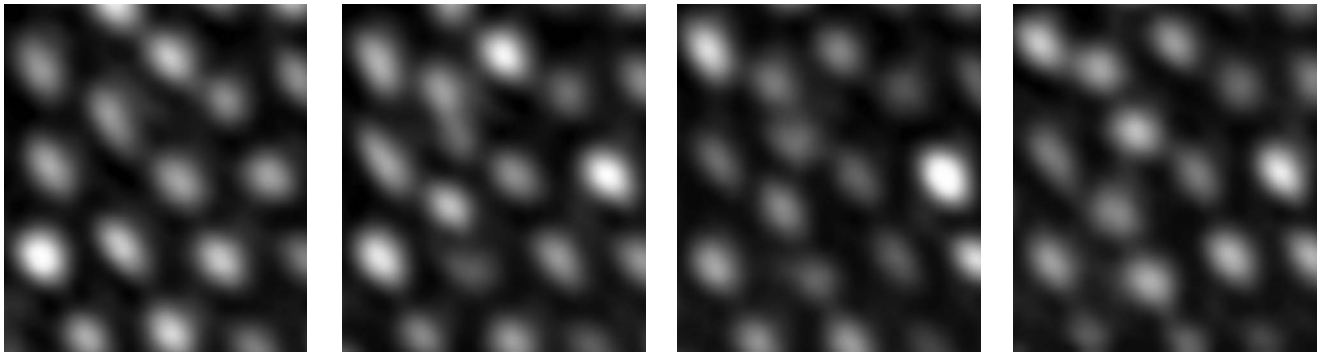

FIG. 4. Real-time observation of rod-splitting events (second column of spots from left). Snapshots of a 65×74 μm^2 region of a growth pattern taken at time intervals of 7 min. $V=0.035$ μm s^{-1}.

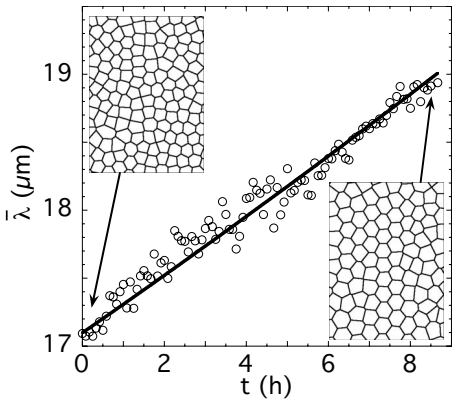

FIG. 5. Time variation of the mean spacing in the absence of rod splittings. $V=0.021\ \mu\mathrm{m\ s}^{-1}$. Open circles: measured values. Continuous line: exponential fit (characteristic time: 82 h). Insets: Voronoi diagrams of a fixed region of the growth pattern at the indicated times. Peaks of a hexagonal structure with dense rows normal to the sample walls progressively appeared in the Fourier transforms of the images (not shown) during the process.

splittings were counted by direct observation (Fig. 4).

Figure 5 shows the time evolution of $\bar{\lambda}$ (defined as the mean value of the nearest-neighbor distances in the Voronoi diagram of the growth pattern) during a period without rod branching of a solidification run. In this example, an exponential (in fact, almost linear) fit yielded $\tau=82\pm12$ h, and hence $R=3.2\pm0.5$ mm, in good agreement with the value of R derived from the measurements of $V_d(y)$ during the same experiment. The same agreement between the two methods of determining R was found in all the experiments. We conclude that the observed stretching of the growth patterns was indeed due to a forward curvature of the isotherms. This should not be a surprise. The isotherms of directional-solidification setups are most commonly curved under the effect of factors such as differences in thermal conductivity between the various materials composing the samples, rejection of latent heat at the growth front, and convection-induced transverse gradients. In our case, the order of magnitude of R ($\approx$10 times as large as the sample thickness) and the fact that R did not depend on V indicate that the curvature of the isotherms was mostly due to the thermal-conductivity inhomogeneity of the samples.

The slow increase in $\bar{\lambda}$ generated by the curved isotherms continued until rod branchings occurred, which reduced $\bar{\lambda}$. The rod branchings mostly took place inside the topological defects of the pattern and contributed to the multiplication of these defects. The global result of this complex interplay was that, after a long solidification time at constant V, the average rod-branching frequency (measured by direct counting) adjusted itself so as to counterbalance the continuous stretching of the growth pattern. We performed a series of solidification rate programs ending with a maintain at constant V, which all led to a long-time dynamics characterized by a plateau in the $\bar{\lambda}(t)$ curve. Illustrative examples are shown in Fig. 6. The fluctuations of $\bar{\lambda}$ over the plateau were due to fluctuations in the ambient conditions and were responsible for a relatively large ($\approx$10%) uncertainty on the plateau spacing value λ_p.

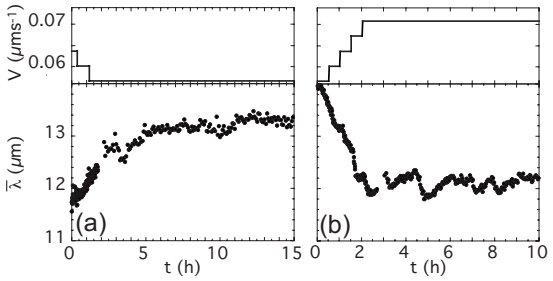

FIG. 6. Time variation of the mean spacing during the solidification rate programs indicated in the upper part of the figure. (a) $\bar{\lambda}_o<\lambda_p$. The transient preceding the plateau is without rod splitting. (b) $\bar{\lambda}_o>\lambda_p$. The rod-branching frequency was initially high and decreased during the transient.

We performed 18 measurements of λ_p in seven different samples, and fitted a $V^{-0.5}$ law onto the data. The best fit value was $\lambda_p/\lambda_m=1.03\pm0.04$ supporting that λ_p was initial-condition independent.

During transients without rod branching, we observed the progressive formation of well-ordered domains separated by sharp boundaries (Fig. 5). The characteristic times of rearrangement were of the same order of magnitude as the phase-diffusion times calculated using the semiempirical formula of Ref. [1]. More surprisingly, the hexagonal arrays inside the domains were oriented with dense rows either parallel or normal to the sample walls, which must be an effect of the stretching of the growth pattern in this direction. This is evidence of the existence of a finite-width stability λ range for the hexagonal growth patterns below λ_p. In this range, disordered patterns relax progressively toward a perfect hexagonal order through phase diffusion and other mechanisms which remain to be identified.

At the end of the transient, rod-branching events occurred in short cascades inside the domain boundaries [9]. This increased the density of topological defects and progressively blurred the structure in domains [10]. A detailed study of this process is beyond the scope of this Brief Report. We limit ourselves to some remarks which cast light on the steady statistical features of the long-time dynamics (Fig. 7). We defined a local spacing λ as the average value of the nearest-neighbor distances of a DC cap, and a local index of stability as the value λ_{sp} of λ at the instant of the splitting. Measurements of λ_{sp} for a large number of events yielded values

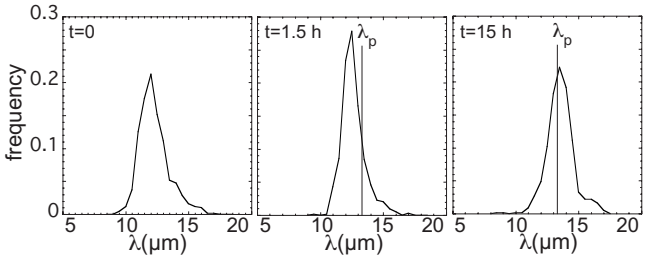

FIG. 7. Normalized histograms of the local spacing at the indicated times during the solidification run of Fig. 6(a). λ_p: mean value at long times. Note that the λ distribution narrowed during the transient, which is due to the formation of well-ordered domains.

ranging from λ_p to $1.25\lambda_p$. These values are those of the peak and maximum values of the statistical distribution of λ at long times, respectively, within the experimental scatter. This suggests that the plateau value λ_p measures the stability limit to rod branching in topological defects while the maximum value of the distribution corresponds the stability limit to rod branching in a hexagonal environment [11].

Finally, these observations also suggest that almost perfect eutectic hexagonal structures could be grown by directional solidification using time-dependent solidification rates. The details of the required process would naturally depend on the specifics of the directional-solidification setup used. In our setup, which is characterized by a slight uniform forward curvature of the isotherm and a quasizero average transverse gradient, the process would basically consist of decelerating the directional solidification in such a way ($dV/dt \approx -2V/\tau$) that the $V^{-0.5}$ increase in λ_p follows, or slightly overtakes, the increase in $\bar{\lambda}$ driven by the curved isotherms. We have tested this concept during relatively short period of times [see Fig. 6(a)] and are currently studying the feasibility of long-duration applications. We note that some of our conclusions are valid *mutatis mutandis* for a backward curvature of the isotherms. Such a curvature would induce a continuous shrinking of the growth pattern and presumably drive the system into a steady long-time dynamics resulting from a competition between curvature-induced shrinking and rod-termination instability. Long transients without rod terminations could be achieved by increasing V [12]. However, the effect on the growth pattern of the injection of rods from the sample walls, which would occur in that case, is unknown.

In conclusion, during the directional solidification of a transparent rodlike eutectic system, we have observed a steady long-time dynamics, which presents statistical features (sharp selection of the mean spacing, broad dispersion of the local spacing values) reminiscent of those observed (but not explained) in metallic eutectics [2]. Broadly speaking, the existence of a steady long-time dynamics is due to a slight instrumental imperfection which drives the system toward a stability boundary of the growth pattern and eventually triggers the corresponding (creation or termination) instability. After a transient, the two processes (external forcing and dynamical instability) come into balance and the mean spacing remains constant although the growth pattern is disordered and nonstationary. Such a conclusion is likely to be of general validity for weakly anisotropic (regular) eutectics.

We thank V. T. Witusiewicz, L. Sturz, and S. Rex from ACCESS (Aachen, Germany) for kindly providing us with purified succinonitrile-(d)camphor alloy. This work was supported by the Centre National d'Etudes Spatiales, France.

[1] S. Akamatsu, M. Plapp, G. Faivre, and A. Karma, Phys. Rev. E **66**, 030501(R) (2002); Metall. Mater. Trans. A **35**, 1815 (2004).

[2] R. Trivedi, J. T. Mason, J. D. Verhoeven, and W. Kurz, Metall. Trans. A **22A**, 2523 (1991).

[3] A. Karma and A. Sarkissian, Metall. Mater. Trans. A **27**, 635 (1996).

[4] M. Ginibre, S. Akamatsu, and G. Faivre, Phys. Rev. E **56**, 780 (1997).

[5] S. Bottin-Rousseau, M. Perrut, C. Picard, S. Akamatsu, and G. Faivre, J. Cryst. Growth **306**, 465 (2007).

[6] K. A. Jackson and J. D. Hunt, Trans. Metall. Soc. AIME **236**, 1129 (1966); the long-lasting conjecture that λ_m is an instability threshold for lamellar eutectic patterns has recently been disproved [1]. Nonetheless, λ_m remains a convenient scaling constant incorporating the (approximate) $\lambda V^{-0.5}$ similarity law of eutectic growth.

[7] S. Akamatsu, S. Bottin-Rousseau, M. Perrut, G. Faivre, L. Sturz, and V. Witusiewicz, J. Cryst. Growth **299**, 418 (2007); also see V. T. Witusiewicz, L. Sturz, U. Hecht, and S. Rex, Acta Mater. **52**, 4561 (2004).

[8] S. Akamatsu, S. Moulinet, and G. Faivre, Metall. Mater. Trans. A **32**, 2039 (2001).

[9] S. Bottin-Rousseau and P. Pocheau, Phys. Rev. Lett. **87**, 076101 (2001); we did not observe any three-dimensional analog of the long-range cascades of splitting events observed by these authors in curved two-dimensional cellular growth fronts.

[10] M. Perrut, Doctoral thesis, University Pierre-et-Marie-Curie, 2007.

[11] The close connection between mean spacing and instability limit reported here is reminiscent of, but actually has a completely different origin than, the "marginal-stability" operating point envisaged in J. S. Langer, Phys. Rev. Lett. **44**, 1023 (1980).

[12] L. Ratke and J. Alkemper, Acta Mater. **48**, 1939 (2000); these authors noted that the degree of order of the hexagonal growth patterns of a directionally solidified Al-Al_3Ni eutectic was tremendously increased by *accelerating* the solidification, but do not give information about the curvature of the isotherms during their experiments.